Journal of Pharmaceutical and Biomedical Analysis 56 (2011) 505–512

Contents lists available at ScienceDirect

Journal of Pharmaceutical and Biomedical Analysis

journal homepage: www.elsevier.com/locate/jpba

Radiolabeling of PAMAM dendrimers conjugated to a pyridine-*N*-oxide DOTA analog with ^{111}In: Optimization of reaction conditions and biodistribution

Veronika Biricová [a], Alice Lázničková [a,*], Milan Lázníček [a], Miloslav Polášek [b], Petr Hermann [b]

[a] Charles University in Prague, Faculty of Pharmacy, Heyrovského 1203, 500 05 Hradec Králové, Czech Republic
[b] Charles University in Prague, Faculty of Science, Department of Inorganic Chemistry, Hlavova 2030, Prague 2, Czech Republic

ARTICLE INFO

Article history:
Received 18 April 2011
Received in revised form 7 June 2011
Accepted 14 June 2011
Available online 22 June 2011

Keywords:
DOTA-pyridine-*N*-oxide derivative
PAMAM conjugates
Indium-111 complexes
Biodistribution studies
Radiopharmaceuticals

ABSTRACT

Polyamidoamine dendrimers (PAMAMs) of generations 1 (G1) and 4 (G4) were conjugated with a bifunctional pyridine-*N*-oxide DOTA analog, 10-[(4-carboxy-1-oxidopyridin-2-yl)methyl]-1,4,7,10-tetraazacyclododecane-1,4,7-triacetic acid (H_4do3a-py^{NO-C}), through the pyridine-4-carboxylic acid group, and the conjugates were radiolabeled with indium-111. Reaction conditions for the radiolabelling were optimized. Both radiolabeled conjugates, G1-[^{111}In(do3a-py^{NO-C})] and G4-[^{111}In(do3a-py^{NO-C})], were kinetically stable for at least 48 h after preparation; in the presence of competitive ligands, the radiochemical purity of the conjugates slightly decreased (4–7%) over the same time period. The preclinical pharmacokinetics of both agents were evaluated. Biodistribution and elimination in rats were more favorable for the G1-[^{111}In(do3a-py^{NO-C})] conjugate than G4-[^{111}In(do3a-py^{NO-C})] conjugate. However, the G1-[^{111}In(do3a-py^{NO-C})] conjugate was rapidly eliminated from the body, mainly through urine, while, significant and long-term radioactivity uptake in the liver and kidney was observed for the G4-[^{111}In(do3a-py^{NO-C})] conjugate.

1. Introduction

Polyamidoamine dendrimers (PAMAMs) have been studied as potential drug carriers, gene delivery carriers and moieties for modification of drug solubility and/or absorption for a many years [1–11]. Conjugation of these dendritic polymers with metal chelators and subsequent complexation with metal ions have led to a range of magnetic resonance imaging contrast agents (MRI CA) [12–21]. Radiolabeling of conjugates with metal radioisotopes has been employed less frequently, despite the fact that it offers access to macromolecular products with high specific activities that are useable in radiotherapy or for imaging [15,22–25]. To use such metal-containing conjugates in medicine, however, the metal ions must be tightly bound in thermodynamically stable and kinetically inert complexes to prevent their possible release, and subsequent toxicity, in an organism. From this point of view, macrocyclic chelators are commonly preferred. Among them, bifunctional derivatives of DOTA (H_4DOTA = 1,4,7,10-tetraazacyclododecane-*N*,*N*′,*N*″,*N*‴-tetraacetic acid) have been most commonly explored.

A DOTA analog with three acetic acids and one methylpyridine-*N*-oxide pendant arm was previously synthesized, and its gadolinium(III) complex was suggested as a possible MRI contrast agent, because it exhibited a fast exchange of the coordinated water molecule with the bulk water [26]. It was also shown that lanthanide(III) complexes of mono(methylpyridine-*N*-oxide) analogs of DOTA had square-antiprismatic structures where all donor atoms of the ligands were coordinated to the central ion (O_4N_4 donor atom set). A water molecule completed the complex by capping the O_4 plane [27]. Such a structure is common for lanthanide(III) complexes of all DOTA-like ligands.

It has been shown that such a cage-like arrangements of the ligand around a central ion is responsible for the high kinetic inertness of complexes of DOTA-like ligands [28]. The bifunctional variant of the original ligand, 10-[(4-carboxy-1-oxidopyridin-2-yl)methyl]-1,4,7,10-tetraazacyclododecane-1,4,7-triacetic acid (H_4do3a-py^{NO-C}), was synthesized [29] and attached to both PAMAM dendrimers of the 0th to 4th generations [30] and calixarenes [31], and the conjugates were investigated as MRI contrast agents (Fig. 1).

Although gadolinium(III) complexes of PAMAM dendrimer conjugates have been frequently studied as MRI contrast agents [32], research on the other metal ion complexes and complexes of metal radioisotopes has been less common.[24,33–37] Therefore, the aim of this study was optimization of the conditions for radiolabeling of G1-(do3a-py^{NO-C}) and G4-(do3a-py^{NO-C}) conjugates with indium-111 and investigation of the kinetic stability of the radiolabelled products under different conditions. In addition, the pharmacokinetics and biodistribution of the radiolabelled dendrimers

* Corresponding author. Tel.: +420 495067478; fax: +420 495067169.
E-mail addresses: biricv@yahoo.co.uk (V. Biricová), alice.laznickova@faf.cuni.cz (A. Lázničková), milan.laznicek@faf.cuni.cz (M. Lázníček), polasek1@natur.cuni.cz (M. Polášek), petrh@natur.cuni.cz (P. Hermann).

0731-7085/$ – see front matter © 2011 Elsevier B.V. All rights reserved.
doi:10.1016/j.jpba.2011.06.009

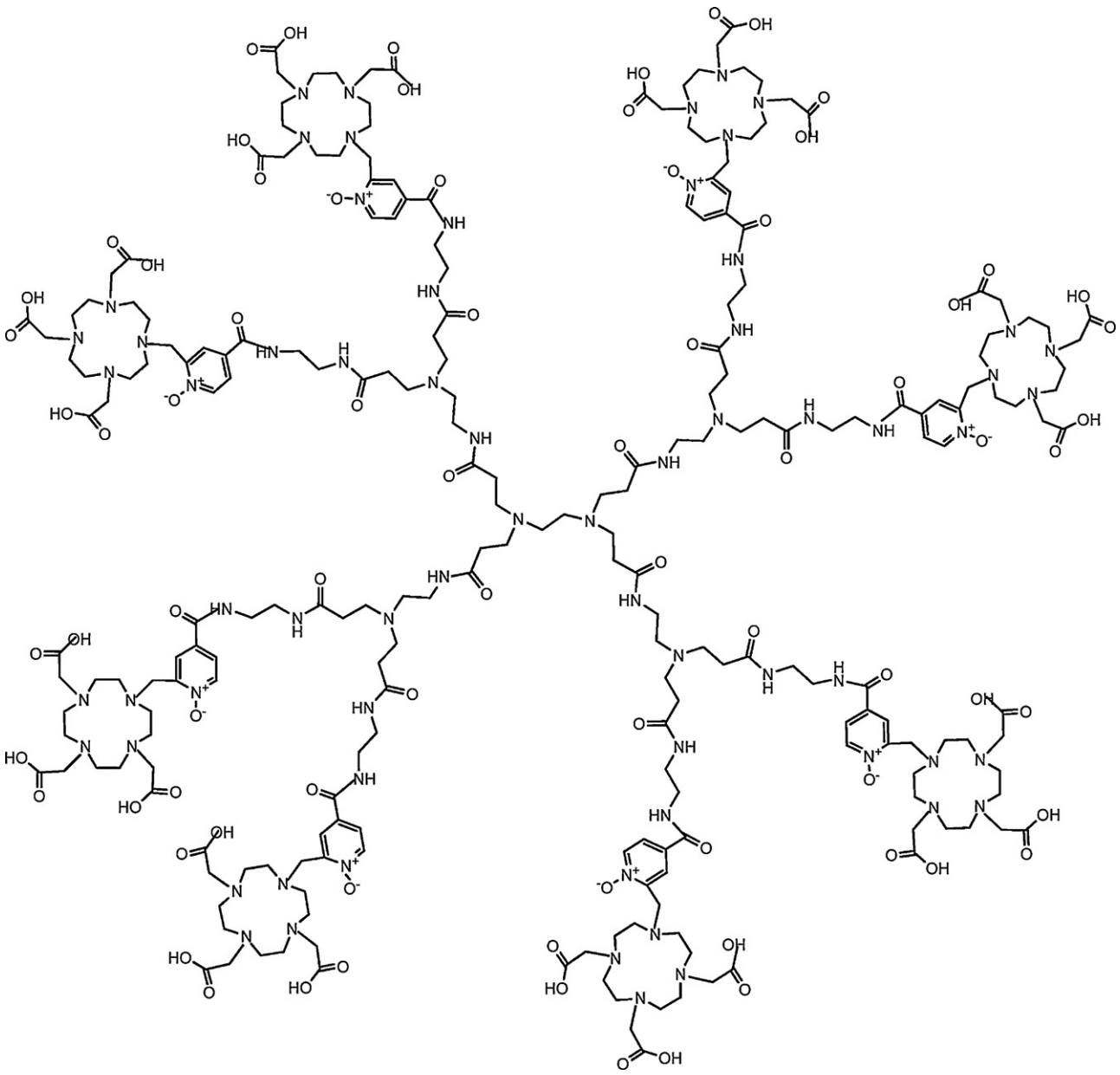

Fig. 1. G1-do3a-py^{NO-C}.

were evaluated to determine the fate of the polymers in the body.

2. Material and methods

2.1. Chemicals and material

The PAMAM conjugates, G1-do3a-py^{NO-C} and G4-do3a-py^{NO-C}, were available from a previous report [30]. The G1-do3a-py^{NO-C} conjugate contained 7.5 complexing moieties per polymer molecule on average (effective M_w = 5266 g/mol), and the G4-do3a-py^{NO-C} conjugate has an average of 57 complexing moieties per polymer molecule (effective M_w = 33,870 g/mol). Special attention was paid to ensure an extra-low content of metal impurities in all of the reagents and laboratory equipment that were used. Deionized water was used throughout the experiments. Sephadex G-25(medium) was received from Sigma–Aldrich and indium(III) chloride hydrate (39% of In) was obtained from Fluka. The other chemicals used in this work were purchased from commercial sources in an appropriate purity and were used as obtained. The radioisotope $^{111}InCl_3$ was purchased from Perkin Elmer Life and Analytical Sciences (Boston, U.S.A.). Animal studies were carried out on male Wistar rats weighing between and 260 g. The animals were fasted overnight before the experiment (to empty the bowels) but had free access to water. The rats were maintained during the experiment in standard animal facilities that complied with the European Convention for the Protection of Vertebrate Animals Used for Experimental and Other Scientific Purposes and all animal experiments were approved by the Ethics Committee of the Faculty of Pharmacy, Charles University in Prague.

2.2. Methods

2.2.1. TLC

Instant thin-layer chromatography (ITLC) of radiolabelled conjugates was performed using silica gel (SG) impregnated glass

fiber sheets (Pall Corporation, U.S.A.) as the solid phase and 0.1 M ammonium acetate with 10 mM EDTA (pH* 5.5) as the mobile phase. After elution, the ITLC-SG strips were dried thoroughly and analyzed with a VZ.15 TLC-analyzer [(TLC-Raytest with RITA detector (Beta-Radioactivity Intelligent Thin Layer Analyzer)] using Rita Control software. The chromatograms were visualized using Gina-Star TLC™ software (version 2.18, Raytest). In this mobile phase, the R_f value of the radiolabeled G1/G4-[^{111}In(do3a-py^{NO-C})] conjugates was 0.1 and the R_f of the free radioisotopes was in the range of 0.9–1. The error in measurements of the purity of the complexes was approximately ±3%.

2.2.2. SEC

Size-exclusion chromatography (SEC) was performed using clean glass columns (30 cm × 1.1 cm) filled with Sephadex G-25(medium) in an aqueous solution as the solid phase and a 0.9% aq. solution of NaCl as the mobile phase. The radioactivity of the collected fractions was measured using an automatic gamma counter 1480 Wizard. SEC was also performed with a TSK gel G2000 PW (7.5 nm × 30 cm, 12 μm, TOSOH Bioscience) column on an Agilent system 1100 Series composed of a degasser (G1322A), a quaternary pump (G1311A), an autosampler (ALS G1313A), a thermostatted column compartment (COLCOM G1316A) and a UV–VIS detector (MWD G1365B), operated with Agilent ChemStation Rev.B.03.02(341). The HPLC system was coupled with a radioactivity detector (CRYTUR, 743114 SKG) and data collector (Universal Laboratory Ratemeter, URL-2 POLON) operating with the software Clarity. Isocratic elution with 0.1 M citric acid buffer with 0.025% sodium azide at a flow rate of 0.8 ml/min was used. The pH of the mobile phase was adjusted to 2.74 using NaOH [38]. The sample concentration was approximately 0.2 μg/μl of conjugate with an injection volume of 100 μl. The sample always contained excess DTPA to prevent the cumulation of free In^{3+} in the chromatographic column. The column temperature was maintained at 25 ± 0.1 °C.

2.2.3. Radiometal–ligand chelation

2.2.3.1. Comparison of radiolabeling efficacy using three different buffers at different pH. A 0.2 M sodium acetate buffer (pH: 3.8, 4.2, 4.6, 5.0 and 5.6), a 0.2 M sodium citrate buffer (pH: 2.2, 3.2, 4.2 and 5.0) and a 0.2 M sodium/potassium phosphate buffer (pH: 5.0, 5.5 and 6.5) were used to understand the efficacy of conjugate radiolabeling. The ligand-PAMAM conjugate stock solution (0.5 μL) was added to 50 μl of one of the three types of buffer with only one chosen pH value. Next, the appropriate amount of $InCl_3$ stock solution (1 equiv. relative to the ligand molecules on the surface of PAMAM dendrimers) spiked with ^{111}In was added to the reaction mixture. The molar concentrations of all components in the reaction tubes are given in Table 1. The final volumes varied from 55 μl to 60 μl according to the concentrations of the stock metal solutions. The reaction mixtures were stirred and incubated at 40 °C up to 4 h. In the meantime, 1 μl of each mixture was analyzed by ITLC 15, 30, 60, 120 and 240 min after mixing.

2.2.3.2. Comparison of radiolabeling efficacy at different temperatures. The 0.2 M sodium acetate buffer (pH 5.0) was chosen to follow the radiolabeling process at 4 different temperatures. The reaction mixtures were incubated for up to 24 h at the chosen temperature, (i.e., 25 °C, 30 °C and 37 °C). Then, 1 μl of each reaction mixture was analyzed by ITLC at the time points 5, 15, 30, 60, 120 and 240 min and 24 h after mixing.

2.2.3.3. Preparation and purification of radiolabeled conjugates. Each conjugate [51 μg; corresponding to 69.2 nmol of ligand for G1-(do3a-py^{NO-C}) and 59.2 nmol of ligand for G4-(do3a-py^{NO-C})] was separately mixed with the 0.2 M sodium acetate buffer solution (pH 5.0, 10 μmol), and freshly prepared In^{3+} solution in 0.04 M HCl was added to each reaction mixture in the molar ratio do3a-py^{NO-C} moiety to In^{3+} of 1:1.2. Radioactivity of an individual sample depended on the isotope decay time. Reaction mixtures were incubating at 30 °C [G1-(do3a-py^{NO-C})] and 37 °C [G4-(do3a-py^{NO-C})] overnight. After the incubation, a DTPA aq. solution [10^{-2} M; 830 μl for G1-(do3a-py^{NO-C}), 710 μl for G4-(do3a-py^{NO-C})] was added, and the mixtures were stirred at room temperature for 2 h. In the samples, the molar ratio of DTPA to metal ion was always 1:100. Then, the reaction mixtures were purified by SEC using a 30 cm × 1.1 cm glass column filled with Sephadex G-25(medium). The purified radiolabeled conjugates (the most radioactive macromolecular fraction/s) were thus analyzed by SEC (to prove the purity and separation efficacy) using a clean glass column (30 cm × 1.1 cm) with Sephadex G-25(medium). Purified products were kept at room temperature and their stabilities were studied by SEC on an Agilent system.

2.2.3.4. Kinetic stability of radiolabelled conjugates. Radiolabeled conjugates were prepared under the optimal conditions for radiolabeling as given above. After finishing the reaction, the purity of the radiolabeled conjugates was analyzed, and their stability at room temperature was checked after 1, 2, 4, 24 and 48 h by ITLC. The results were also confirmed by SEC on an Agilent system after 0, 24 and 48 h of standing at room temperature. Radiolabelled conjugates were pre-purified on the Sephadex column before injection onto the HPLC chromatographic column. Aqueous solutions of purified conjugates were mixed with fresh rat plasma in the volume ratio of 1:1 and incubated for 48 h at 37 °C. Their radiochemical purity was determined by SEC on a TSK gel column after the filtration through a Teknokroma syringe filter (PTFE, 0.22 μm, TR-200503, 13 mm PK/100) at the time points 0, 1, 2, 4, 24 and 48 h after mixing.

2.2.3.5. Kinetic stability of radiolabeled conjugates in the presence of competitive chelators. Radiolabeled conjugates G1-[^{111}In(do3a-py^{NO-C})] or G4-[^{111}In(do3a-py^{NO-C})] (approximately 0.4 nmol) were mixed with the aq. solutions of the competitive ligands (DTPA or EDTA, 2.5 mM, pH 6.5, 16 μl) in the surface do3a-py^{NO-C} to DTPA/EDTA molar ratio of 1:100, and the resulting solutions were kept at room temperature. The stability of the conjugates was determined by ITLC after 0, 1, 2, 4, 24 and 48 h.

2.2.4. Pharmacokinetic studies

2.2.4.1. Distribution studies. Radiolabeled G1-[(^{111}In(do3a-py^{NO-C})] and G4-[(^{111}In(do3a-py^{NO-C})] were administered to rats intravenously in a volume of 0.2 ml (1.5 μg/ml). At 5 min, 1, 2, 24 and 48 h after dosing, the carotid artery was exposed under ether anesthesia, and a blood sample was collected in a glass tube containing dry heparin. After exsanguination, the tissues and organs of interest were removed and weighed, and their radioactivity was measured in a Wizard 3 gamma counter (Perkin Elmer).

2.2.4.2. Elimination studies. The agents under study were administered to rats as described above. Following administration, the animals were placed into separate glass metabolic cages, the construction of which allowed reliable separation of the urine and solid excrements. The animals had free access to standard diet and water. Two hours after administration, the rats were forced to empty their urinary bladders by handling (immobilization) and urine and feces were collected. The procedure was repeated at 24 h and 48 h intervals after administration.

3. Results and discussion

The dendrimer conjugates used here, G1-(do3a-py^{NO-C}) and G4-(do3a-py^{NO-C}), were prepared previously [30] and contained

Table 1
Molar amounts of the compounds used for radiolabeling.

Molar amount	G1-(do3a-py^{NO-C})	G4-(do3a-py^{NO-C})
NaOAc [μmol]	10	10
Na citrate [μmol]	10	10
Na/K phosphate [μmol]	10	10
Surface ligand (do3a-py^{NO-C}) [nmol]	35	30
$InCl_3 \pm {}^{111}InCl_3$ [nmol]	35	30
Activity [mCi, MBq]	0.05 ± 0.003 mCi (1.85 ± 0.11 MBq)	0.05 ± 0.003 mCi (1.85 ± 0.11 MBq)
HCl [nmol]	110	110

an average of 7.5 (ideally 8) and 57 (ideally 64) complex units per conjugate molecule, respectively. For characterizing the formation of the complex, we investigated conditions for radiolabeling of dendrimers with attached metal-binding moieties in diluted radionuclide solution. Indium-111 was chosen as a good model metal radioisotope.

3.1. Optimization of reaction conditions

The influences of buffer type, pH value and reaction temperature on the radiochemical yield were investigated, and the purity of the final radiolabeled conjugates was measured. Three different buffers having different pH values were chosen according to their buffering capacity to follow the efficacy of the conjugate radiolabeling. A non-radioactive solution of $InCl_3$ spiked with the radioactive isotope (^{111}In), was used to fully saturate the free ligand groups on the surface of the dendrimers. As expected, the complexation progress depended on the type of buffer and its pH value. Citrate buffer acts as a weak chelator, so the radiolabeling of the conjugates was slow. A strong pH dependence was observed: at low pH (pH 2.2), indium(III) is hardly complexed by the ligands as the metal ion and protons competed for the same binding sites (oxygen and nitrogen donor atoms) of the DO3A-py^{NO-C}. Furthermore, citrate as a pure oxygen donor competed effectively with the macrocycle for indium(III) binding under these acidic conditions. Even at higher pH (>3.2), the citrate buffer still significantly slowed the In(III)-DO3A-py^{NO-C} complex formation, as the macrocyclic complex formation was a transchelation under these conditions. However, hydrolysis of indium(III) started to play a significant role in the total complexation efficacy at the highest pH values. Phosphate buffer was also not appropriate for radiolabeling of the conjugates with In-111 as it precipitated as insoluble $InPO_4$. However, the DO3A-py^{NO-C} was such a strong chelator for trivalent indium that it was seen to pull the indium(III) from the precipitated $InPO_4$ after longer incubation times.

The most suitable buffer for the complexation of indium(III) ions by the conjugates seemed to be acetate buffer (Fig. 2(A)). The pure metal-loaded conjugates were formed quickly over a broad pH range, even though trivalent indium starts to hydrolyze at pH values over 2.5. In this medium, weak complexation by the acetate anions partially prevented the precipitation, and the strong macrocyclic ligand was able to bind the metal ion in acidic solutions. The effect of the dendrimer cores could also be important as their amide groups were able to weakly complex the highly charged metal ion and thus prevent precipitation and help to bring the metal ion close to the strongly complexing macrocyclic moiety.

The small influence of reaction pH on complexation yield in the acetate buffer was more obvious for the radiolabeling of the larger G4-(do3a-py^{NO-C}) conjugate. Due to the higher density of ligand moieties on the surface of the G4-conjugate, the complexation reaction was even faster than for the G1-conjugate, while the effect of indium(III) hydrolysis was insignificant. Thus, the most suitable conditions for radiolabeling of both G1-(do3a-py^{NO-C}) and G4-(do3a-py^{NO-C}) conjugates with the carrier-added In-111 were those employing acetate buffer at pH 5.0 (Fig. 2(A)).

Under the optimal pH of 5.0, the influence of temperature was monitored to obtain the purest forms of the complexes possible. Progress in binding of In(III) by the conjugate moieties was studied up to 24 h at 25 °C, 30 °C and 37 °C. The temperature has an impact on the complexation reaction. Fortunately, the reaction progressed quickly enough for the purposes of this study at 30 °C, which was a suitable temperature for biomolecules, such as protein structures or antibodies, that could possibly be modified with a dendrimer-ligand conjugate. The higher temperature accelerated the binding. After 2 h, full complexation was reached, even at 25 °C in the case of G4-[^{111}In(do3a-py^{NO-C})] and at 30 °C in the case of G1-[^{111}In(do3a-py^{NO-C})] (Fig. 2(B)). Under optimal conditions for the reaction (0.2 M acetate buffer, pH 5.0), the G1-[^{111}In(do3a-py^{NO-C})] and G4-[^{111}In(do3a-py^{NO-C})] conjugates were obtained in radiochemical purity above 95% (Fig. 3(A)). A longer incubation (24 h) did not significantly improve complex formation yield, but we still suggest incubating over-night to make certain that the complex is completely formed.

The above data showed that pure radiolabeled conjugates could be obtained from the optimized reaction conditions and that these conjugates were suitable for the following experiments.

3.2. Stability experiments

Another goal of this study was to follow the kinetic stability of the radiolabeled conjugates. The complex moieties on the surface of the dendrimeric conjugates were fully stable for at least 48 h at room temperature according to ITLC-SG analysis (Table 2). The radiochemical purity of the G1-[^{111}In(do3a-py^{NO-C})] and G4-[^{111}In(do3a-py^{NO-C})] conjugates was also determined by size-exclusion chromatography (SEC) after 0, 24 and 48 h of storage as their aqueous solutions at room temperature (Fig. 3(B)). All three peaks in the figures had the same profile; there were no peak(s) corresponding to any impurities at any time in the analysis. The largest peak corresponded to the radiolabeled conjugate just after purification by SEC on Sephadex G-25 using a glass column. The middle and the smallest peaks belonged to the radiolabeled conjugate after 24 h and 48 h of storage, respectively. After the correction of the results for the decay factor, we observed that the areas under the peaks decreased due to weakening radioactivity according to the half-life of the radioisotope (2.83 d) (Fig. 3(B)). The radiochemical purity of both conjugates incubated at 37 °C with rat plasma slightly decreased (~3%) (Table 2).

Kinetic stability of the G1-[^{111}In(do3a-py^{NO-C})] and G4-[^{111}In(do3a-py^{NO-C})] conjugates was also tested in the presence of competitive ligands. In the presence of 100-fold excess EDTA, a small loss of radiolabel took place, manifested as a decrease of 3–4% in the radiochemical purity of the radiolabeled conjugates after 48 h (Table 2). As the error in measurements of complex purity determined by TLC was ±3%, the more important results were those obtained using DTPA as a competitive ligand. The radiochemical purity of both G1-[^{111}In(do3a-py^{NO-C})] and G4-[^{111}In(do3a-py^{NO-C})] decreased by approximately ~7% after 48 h of incubation, as DTPA is a stronger chelator for indium(III) than EDTA

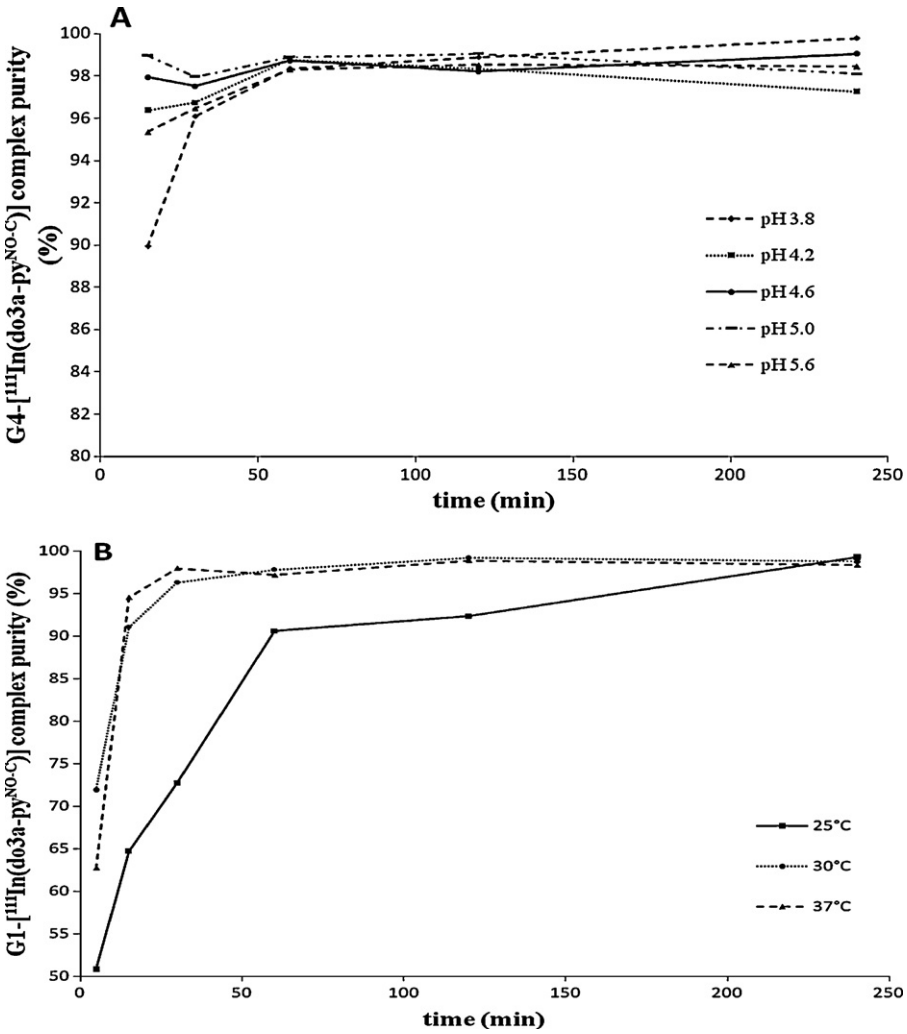

Fig. 2. Dependence of the G4-[^{111}In(do3a-py^{NO-C})] complex formation yield on pH: (A) 0.2 M sodium acetate buffer. Formation yield of the G1-[^{111}In(do3a-py^{NO-C})] complex at different temperatures: (B) 0.2 M acetate buffer, pH 5.0. Ligand moiety: metal ion molar ratio of 1:1; $c_{G1\text{-}(do3a\text{-}py^{NO-C})} = 8.5 \times 10^{-5}$ M (corresponding to $c_{do3a\text{-}py^{NO-C}} = 6.4 \times 10^{-4}$ M); $c_{G4\text{-}(do3a\text{-}py^{NO-C})} = 1.42 \times 10^{-5}$ M (corresponding to $c_{do3a\text{-}py^{NO-C}} = 8.1 \times 10^{-4}$ M); 40 °C.

(Table 2). This result indicated a probable incomplete formation of the complex between the DOTA-like ligand and In^{3+}.

To confirm that the conjugates were suitable for biological experiments, stability experiments in DTPA medium were repeated with radiolabeled conjugates purified by GPC on Sephadex G-25(medium) (Fig. 4). In this case, the complex seemed to be kinetically stable, so the radiolabeled conjugates were suitable for pharmacokinetic and biodistribution studies in rats.

3.3. Pharmacokinetic studies

To have initial data on the fate of our dendrimers in living organisms, we undertook biodistribution studies in rats. The results are summarized in Fig. 5. The G1-[^{111}In(do3a-py^{NO-C})] conjugate displayed a relatively fast blood radioactivity clearance, with only 0.51 ± 0.07% administered dose remaining in the blood 2 h after injection. A high radioactivity uptake in the kidney in the shortest time intervals after dosing was evidently connected with elimination of the agent to urine. Radioactivity identified at the longer time intervals in the bowels was caused by a partial elimination of the radioactivity to feces (Table 3). No specific radioactivity retention in other organs or tissues was found.

For G4-[^{111}In(do3a-py^{NO-C})], a slower blood radioactivity time decrease was observed. Two hours after administration, 4.33 ± 0.70% of the administered activity was still in the bloodstream. Contrary to the G1-[^{111}In(do3a-py^{NO-C})] conjugate,

Table 2
Kinetic stability of G1/G4-[^{111}In(do3a-py^{NO-C})] conjugates in water, rat plasma and in the presence of 100-fold molar excess of EDTA or DTPA.

Time	Radiochemical purity [%]							
	G1	G4	G1 ± plasma	G4 ± plasma	G1 ± EDTA	G4 ± EDTA	G1 ± DTPA	G4 ± DTPA
0 h	98.0	99.9	95.2	99.3	97.0	99.9	98.0	99.9
1 h	98.3	99.2	94.6	–	97.0	96.4	96.7	98.1
2 h	98.4	98.7	95.2	97.0	96.9	97.7	96.8	97.6
4 h	99.0	99.4	93.6	–	96.9	95.6	98.4	93.7
24 h	98.6	98.2	93.1	96.1	94.4	96.7	98.5	96.8
48 h	97.7	98.7	92.3	96.2	94.4	95.8	91.0	93.1

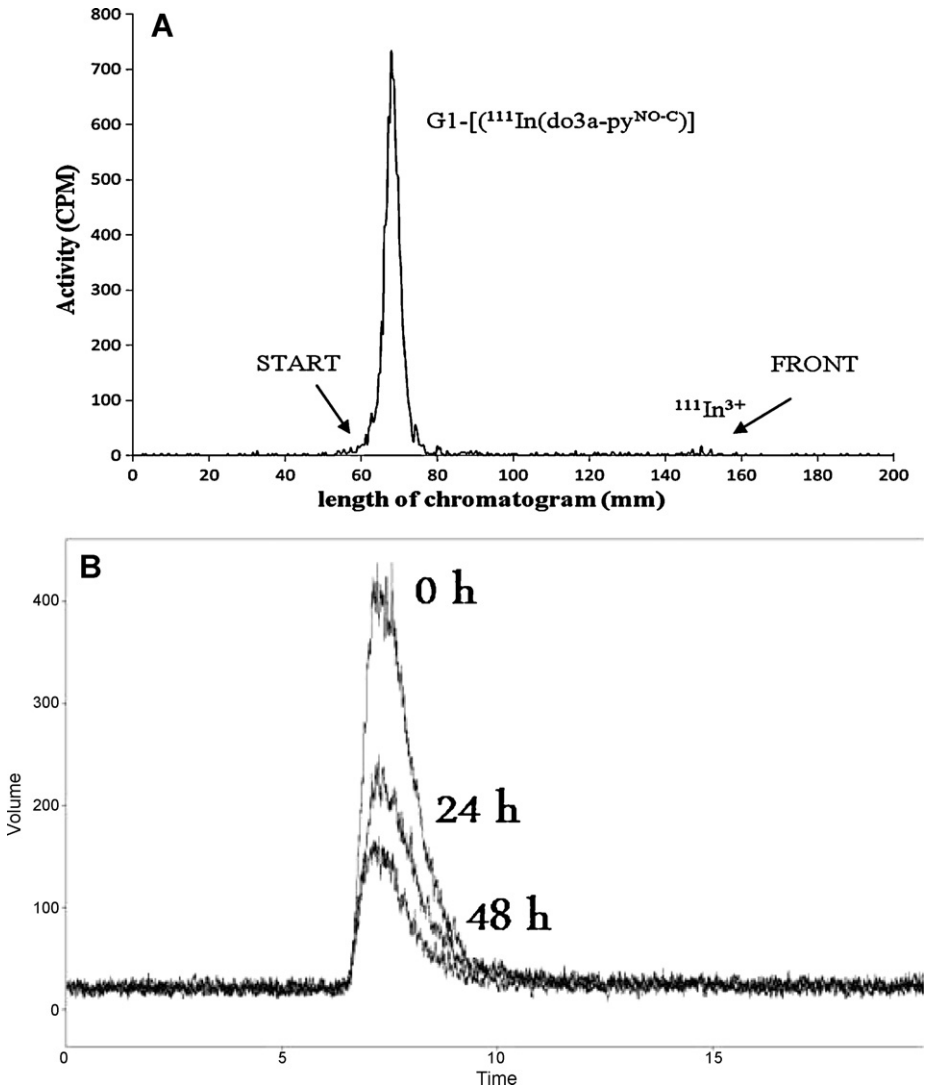

Fig. 3. An example of ITLC analysis of G1-[^{111}In(do3a-py^{NO-C})]; mobile phase: 0.1 M ammonium acetate with 10 mM EDTA, pH 5.5 (A). SEC profiles of the G4-[^{111}In(do3a-py^{NO-C})] conjugate after 0, 24 and 48 h of storage as an aqueous solution at room temperature (B).

G4-[^{111}In(do3a-py^{NO-C})] administration led to high and long-term radioactivity uptake in the liver and kidneys. Specifically, 20.56 ± 2.59% and 5.85 ± 0.58% of the administered radioactivity was still present in the liver and kidneys 48 h post-injection, respectively. The main elimination pathway for G1-[^{111}In(do3a-py^{NO-C})] was its excretion to urine (Fig. 5(A)) but in the case of G4-[^{111}In(do3a-py^{NO-C})], less than one half of the administered radioactivity was eliminated from the body after 48 h (mostly by urine), and a significant portion of radioactivity still remained in the body (Fig. 5(B)).

Radioactivity excreted by urine was mostly in the parent form. From 60.9% of total activity eliminated during 24 h after administration of G1-[^{111}In(do3a-py^{NO-C})] to rats, 98.8% of total urine radioactivity collected in the interval 0–2 h after administration and 91.5% of total urine radioactivity collected in the interval 2–24 h after administration was in the parent form. From 35.1% of total activity eliminated during 24 h after administration of G4-[^{111}In(do3a-py^{NO-C})] to rats, 93.4% of total urine radioactivity collected in the interval 0–1 h after administration and 73.7% of total urine radioactivity collected in the interval 1–2 h after administration was in the parent form. However, the chemical form of radioactivity accumulated in the liver and kidneys is of unknown species. Its specification will need further study.

Free ^{111}In-do3a-py^{NO-C} chelator was expected to be rapidly excreted in urine as a degradation product [39], but this possible metabolite was not a serious obstacle to the diagnostic and therapeutic use of radiolabeled dendrimer-modified biomolecules. The open question about the biological behavior of

Table 3
Elimination results of G1-[^{111}In(do3a-py^{NO-C})] and G4-[^{111}In(do3a-py^{NO-C})] (%ID ± SD) in rats.

% I.D.	G1-(do3a-py^{NO-C})		G4-(do3a-py^{NO-C})	
	urine	*feces*	*urine*	*feces*
2 h	29.70 ± 12.53	–	20.61 ± 6.70	–
24 h	56.26 ± 9.42	8.80 ± 7.69	32.02 ± 6.57	3.98 ± 3.60
48 h	60.91 ± 8.17	11.75 ± 9.38	35.06 ± 6.50	5.19 ± 4.89

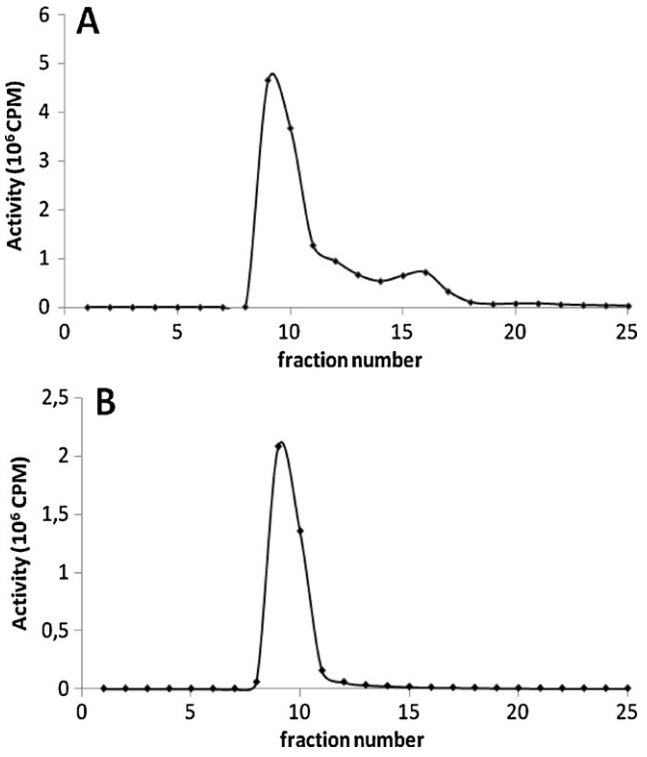

Fig. 4. Example of GPC purification (A) and GPC analysis (B) of G1-[(^{111}In(do3a-py^{NO-C})]. Separation was accomplished on a glass column (30 cm × 1.1 cm; solid phase: Sephadex G-25(medium); mobile phase: 0.9% aq. NaCl).

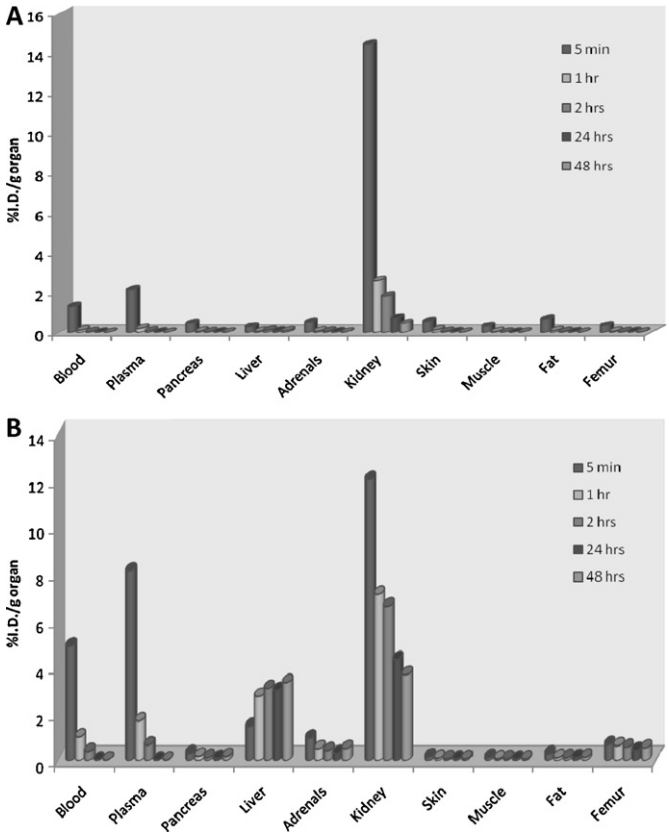

Fig. 5. Biodistribution data for [^{111}In(G1-do3a-py^{NO-C})] (A) and G4-[^{111}In(do3a-py^{NO-C})] (B) (% ID/g organ ± SD) in rats.

the radiolabeled dendrimers, G1-[(^{111}In(do3a-py^{NO-C})] and G4-[(^{111}In(do3a-py^{NO-C})], remains, if they might dissociate from the targeted biomolecules in the body. Therefore, preclinical determination of distribution profiles of G1-[(^{111}In(do3a-py^{NO-C})] and G4-[(^{111}In(do3a-py^{NO-C})] formed part of this study. From a radiochemical point of view, the G4-[^{111}In(do3a-py^{NO-C})] conjugate was more suitable for radiolabeling of biomolecules than G1-[^{111}In(do3a-py^{NO-C})], as the G4-do3a-py^{NO-C} conjugate bears a large number of chelating units. These units allow the attachment of more metal radioisotopes to a single biomolecule (e.g., antibody). However, from a pharmacokinetic point of view, the distribution profile of G4-[^{111}In(do3a-py^{NO-C})] was very unfavorable. The high and long-term radioactivity uptake in the liver and kidneys limited the prospects of G4-(do3a-py^{NO-C}) for radiolabeling of target-specific biomolecules. For nuclear medicine applications, the G1-(do3a-py^{NO-C}) conjugate seemed to be a more promising agent for an attachment of a large number of metal radioisotopes to a single biomolecule than G4-(do3a-py^{NO-C}).

4. Conclusion

In our study, PAMAM dendrimers of the 1st and 4th generation with H_4do3a-py^{NO-C} ligands on their surface were radiolabeled with In-111 and tested. The radiolabeling was successfully performed at a temperature acceptable for sensitive biomolecules (37 °C). The radiolabeled conjugates were purified on a Sephadex SEC column on a preparative scale for further utilization. Our study demonstrates a high stability of ^{111}In labeled conjugates, G1-[^{111}In(do3a-py^{NO-C})] and G4-[^{111}In(do3a-py^{NO-C})]. Radiolabeled species were stable in rat plasma for 48 h. In the presence of EDTA/DTPA competitors, the radiochemical purity of the conjugates slightly decreased over the same time period. Dendrimer-ligand conjugates under this study are thus promising agents for radiolabeling of monoclonal antibodies and their fragments to achieve a high specific activity. Highly branched dendrimers with a maximum number of metal chelators on their surface are favorable for these purposes. Preliminary analysis of biodistribution and elimination characteristics of both radiolabeled conjugates in rats indicated more favorable pharmacokinetic properties of G1-[^{111}In(do3a-py^{NO-C})] in comparison with G4-[^{111}In(do3a-py^{NO-C})]. The latter dendrimer exhibited high and long term radioactivity accumulation in the liver and kidneys. This finding limits the use of G4-[^{111}In(do3a-py^{NO-C})] in nuclear medicine. Radioactivity of both agents under this study was eliminated from the body mostly by urine mainly in the parent form.

Acknowledgements

This project was financially supported by the Grant Agency of Charles University (No. 111008), Grant the Agency of the Czech Republic (P304/10/1738 and No. 203/09/1056), the Ministry of Education of the Czech Republic (No. OC08006), and the grant SVV-2010-261-001. The work was done in frame with BM0607 COST Actions.

References

[1] Z. Dong, H. Katsumi, T. Sakane, A. Yamamoto, Effects of polyamidoamine (PAMAM) dendrimers on the nasal absorption of poorly absorbable drugs in rats, Int. J. Pharm. 393 (2010) 245–253.
[2] K. Borowska, B. Laskowska, A. Magoń, B. Mysliwiec, M. Pyda, S. Wolowiec, PAMAM dendrimers as solubilizers and hosts for 8-methoxypsoralene enabling transdermal diffusion of the guest, Int. J. Pharm. 398 (2010) 185–189.
[3] M. Ma, Y. Cheng, Z. Xu, P. Xu, H. Qu, Y. Fanq, T. Xu, L. Wen, Evaluation of polyamidoamine (PAMAM) dendrimers as drug carriers of anti-bacterial drugs using sulfamethoxazole (SMZ) as a model drug, Eur. J. Med. Chem. 42 (2007) 93–98.
[4] N. Man, Y. Cheng, T. Xu, D. Yang, W. Xiaomin, L. Zhenwei, Ch. Zhichao, H. Guanyi, S. Yunyu, W. Longping, Dendrimers as potential drug carriers. Part II. Prolonged

delivery of ketoprofen by in vitro and in vivo studies, Eur. J. Med. Chem. 41 (2006) 670–674.
[5] Y. Cheng, M. Li, T. Xu, Potential of poly(amidoamine) dendrimers as drug carriers of camptothecin based on encapsulation studies, Eur. J. Med. Chem. 43 (2008) 1791–1795.
[6] D. Chandrasekar, R. Sistla, F.J. Ahmad, R.K. Khar, P.V. Diwan, The development of folate-PAMAM dendrimer conjugates for targeted delivery of anti-arthritic drugs and their pharmacokinetics and biodistribution in arthritic rats, Biomaterials 28 (2007) 504–512.
[7] A.E. Beezer, A.S.H. King, I.K. Martin, J.C. Mitchel, L.J. Twyman, C.F. Wain, Dendrimers as potential drug carriers; encapsulation of acidic hydrophobes within water soluble PAMAM derivatives, Tetrahedron 59 (2003) 3873–3880.
[8] Y. Cheng, H. Qu, M. Ma, Z. Xu, P. Xu, Y. Fanq, T. Xu, Polyamidoamine (PAMAM) dendrimers as biocompatible carriers of quinolone antimicrobials: an in vitro study, Eur. J. Med. Chem. 42 (2007) 1032–1038.
[9] X. Shi, I.J. Majoros, J.R. Baker, Capillary electrophoresis of poly(amidoamine) dendrimers: from simple derivatives to domplex multifunctional medical nanodevices, Mol. Pharm. 2 (4) (2005) 278–294.
[10] B. Klajnert, M. Sadowska, M. Bryszewska, The effect of polyamidoamine dendrimers on human erythrocyte membrane acetylcholinesterase activity, Bioelectrochemistry 65 (1) (2004) 23–26.
[11] L. Zhou, L. Gan, H. Li, X. Yang, Studies on the interactions between\ DNA and PAMAM with fluorescent probe $[Ru(phen)_2dppz]^{2+}$, J. Pharm. Biomed. Anal. 43 (2007) 330–334.
[12] K. Nwe, D. Milenic, L.H. Bryant, C.A.S. Regino, M.W. Brechbiel, Preparation, characterization and in vivo assessment of Gd-albumin and Gd-dendrimer conjugates as intravascular contrast-enhancing agents for MRI, J. Inorg. Biochem. 105 (2011) 722–727.
[13] K. Luo, G. Liu, B. He, Y. Wu, Q. Gong, B. Song, H. Ai, Z. Gu, Mutifunctional gadolinium-based dendritic macromolecules as liver targeting paging probes, Biomaterials 32 (2011) 2575–2585.
[14] L. Han, J. Li, S. Huang, R. Huang, S. Liu, X. Hu, P. Yi, D. Shan, X. Wang, H. Lei, Ch. Jiang, Peptide-conjugated polyamidoamine dendrimer as a nanoscale tumor-targeted T1 magnetic resonance imaging contrast agent, Biomaterials 32 (2011) 2989–2998.
[15] H. Kobayashi, S. Kawamoto, T. Saga, N. Sato, T. Ishimori,J. Konishi, K. Ono, K. Togashi, M.W. Brechbiel, Avidin-dendrimer-$(1B4M\text{-}Gd)_{254}$: a tumor-targeting therapeutic agent for gadolinium neutron capture therapy of intraperitoneal disseminated tumor which can be monitored by MRI, Bioconjugate Chem. 12 (2001) 587–593.
[16] J. Rudovský, M. Botta, P. Hermann, K.I. Hardcastle, I. Lukeš, S. Aime, PAMAM dendrimeric conjugates with a Gd-DOTA phosphinate derivative and their adducts with polyaminoacids: the interplay of global motion, internal rotation, and fast water exchange, Bioconjugate Chem. 17 (2006) 975–987.
[17] S. Svenson, D.A. Tomalia, Dendrimers in biomedical applications—reflections on the field, Adv. Drug Deliv. Rev. 57 (2005) 2106–2129.
[18] A.J.L. Villaraza, A. Bumb, M.W. Brechbiel, Macromolecules, dendrimers, and nanomaterials in magnetic resonance imaging: the interplay between size, function, and pharmacokinetics, Chem. Rev. 110 (2010) 2921–2959.
[19] K. Nwe, L.H. Bryant Jr., M.W. Brechbiel, Poly(amidoamine) dendrimer based MRI contrast agents exhibiting enhanced relaxivities derived via metal preligation techniques, Bioconjugate Chem. 21 (2010) 1014–1017.
[20] K. Nwe, H. Xu, C.A.S. Regino, M. Bernardo, L. Ileva, L. Riffle, K.J. Wong, M.W. Brechbiel, A new approach in the preparation of dendrimer-based bifunctional diethylenetriaminepentaacetic acid MR contrast agent derivatives, Bioconjugate Chem. 20 (2009) 1412–1418.
[21] Z. Jászberényi, L. Moriggi, P.P. Schmidt, C. Weidensteiner, R. Kneuer, A.E. Merbach, L. Helm, E. Tóth, Physicochemical and MR imaging characterisation of Gd3+ loaded PAMAM and hyperbranched dendrimers, J. Biol. Inorg. Chem. 12 (3) (2007) 406–420.
[22] M.W. Brechbiel, Bifunctional chelates for metal nuclides, Q. J. Nucl. Med. Mol. Imag. 52 (2008) 166–173.
[23] C. Wängler, G. Moldenhauer, M. Eisenhut, U. Haberkorn, W. Mier, Antibody-dendrimer conjugates: the number, not the size of the dendrimers, determines the immunoreactivitz, Bioconjugate Chem. 19 (2008) 813–820.
[24] H. Kobayashi, N. Sato, T. Saga, Y. Nakamoto, T. Ishimori, S. Toyama, K. Togashi, J. Konishi, M.W. Brechbiel, Monoclonal antibody-dendrimer conjugates enable radiolabeling of antibody with markedly high specific activity with minimal loss of immunoreactivity, Eur. J. Nucl. Med. 27 (2000) 1334–1339.
[25] S. Sadekar, A. Ray, M. Janat-Amsbury, C.M. Peterson, H. Ghandehari, Comparative biodistribution of PAMAM dendirmers and HPMA copolymers in ovarian-tumor-bearing mice, Biomacromolecules 12 (2011) 88–96.
[26] M. Polášek, J. Rudovský, P. Hermann, I. Lukeš, L.V. Elst, R.N. Muller, Lanthanide(III) complexes of a pyridine-*N*-oxide analogue of DOTA: exclusive *M* isomer formation induced by a six-membered chelate ring, Chem. Commun. 22 (2004) 2602–2603.
[27] M. Polášek, J. Kotek, P. Hermann, I. Císařová, K. Binnemans, I. Lukeš, Lanthanide(III) complexes of pyridine-*N*-oxide analogues of DOTA in solution and in the solid state. A new kind of isomerism in complexes of DOTA-like ligands, Inorg. Chem. 48 (2009) 466–475.
[28] E. Brücher, Kinetic stabilities of Gadolinium(III) chelates used as MRI contrast agents, Top. Curr. Chem. 221 (2002) 103–122.
[29] M. Polášek, M. Šedinová, J. Kotek, L.V. Elst, R.N. Muller, P. Hermann, I. Lukeš, Pyridine-N-oxide analogues of DOTA and their Gadolinium(III) complexes endowed with a fast water exchange on the square-antiprismatic isomer, Inorg. Chem. 48 (2009) 455–465.
[30] M. Polášek, P. Hermann, J.A. Peters, C.F.G.C. Geraldes, I. Lukeš, PAMAM dendrimers conjugated with an uncharged gadolinium (III) chelate with a fast water exchange: the influence of chelate charge on rotational dynamics, Bioconjugate Chem. 20 (2009) 2142–2153.
[31] D.T. Schühle, M. Polášek, I. Lukeš, T. Chauvin, É. Tóth, J. Schatz, U. Hanefeld, M.C.A. Stuart, J.A. Peters, Densely packed Gd(III)-chelates with fast water exchange on a calix[4]arene scaffold: a potential MRI contrast agent, Dalton Trans. 39 (2010) 185–191.
[32] W.C. Floyd, P.J. Klemm, D.E. Smiles, A.C. Kohlgruber, V.C. Pierre, J.L. Mynar, J.M.J. Fréchet, K.N. Raymond, Conjugation effects of various linkers on Gd(III) MRI contrast agents with dendrimers: optimizing the hydroxypyridinonate (HOPO) ligands with nontoxic, degradace esteramide (EA) dendrimers for high relaxivity, J. Am. Chem. Soc. 133 (8) (2011) 2390–2393.
[33] M. Mamede, T. Saga, H. Kobayashi, T. Ishimori, T. Higashi, N. Sato, M.W. Brechbiel, J. Konishi, Radiolabeling of avidin with very high specific activity for internal radiation therapy of intraperitoneally disseminated tumors, Clin. Cancer Res. 9 (2003) 3756–3762.
[34] H. Kobayashi, Ch. Wu, M.-K. Kim, Ch.H. Paik, H.A. Carrasquillo, M.W. Brechbiel, Evaluation of the in vivo biodistribution of indium-111 and yttrium-88 labeled dendrimer-1B4M-DTPA and its conjugation with anti-Tac monoclonal antibody, Bioconjugate Chem. 10 (1999) 103–111.
[35] J.C. Roberts, M.K. Bhalgat, R.T. Zera, Preliminary biological evaluation of polyamidoamine (PAMAM) Starburst™ dendrimers, J. Biomed. Mater. Res. 30 (1996) 53–65.
[36] Ch. Wu, M.W. Brechbiel, R.W. Kozak, O.A. Gansow, Metal-chelate-dendrimer-antibody constructs for use in radioimmunotherapy and imaging, Bioorg. Med. Chem. Lett. 4 (3) (1994) 449–454.
[37] H. Kobayashi, N. Sato, S. Kawamoto, T. Saga, A. Hiraga, T. Ishimori, J. Konishi, K. Togashi, M.W. Brechbiel, 3D MR angiography of intratumoral vasculature using a novel macromolecular MR contrast agent, Magn. Res. Med. 46 (2001) 579–585.
[38] D.A. Tomalia, I.J. Majoros, Biocompatible Dendrimers, US Patent US 7,078,461 B2 (2006).
[39] M. Petřík, A. Lázničková, M. Polášek, Labelling of a bifunctional pyridinoxide derivative of DOTA with In-111 and Y-90: radiochemical aspects and preclinical results, Eur. J. Nucl. Med. Mol. Imag. 34 (2007) 334.